

The CLEAR Experiment

K. Scholberg and T. Wongjirad

Department of Physics, Duke University, Durham, NC 27708, USA

E. Hungerford and A. Empl

Department of Physics, U. of Houston, Houston, TX 77204, USA

D. Markoff

North Carolina Central University, Durham, NC 27695, USA

P. Mueller

Physics Division, Oak Ridge National Laboratory, TN 37831, USA

Y. Efremenko

Department of Physics and Astronomy, U. of Tennessee, Knoxville, TN 37996, USA

D. McKinsey and J. Nikkel

Department of Physics, Yale University, New Haven, CT 06520, USA

The Spallation Neutron Source in Oak Ridge, Tennessee, is designed to produce intense pulsed neutrons for various science and engineering applications. Copious neutrinos are a free by-product. When it reaches full power, the SNS will be the world's brightest source of neutrinos in the few tens of MeV range. The proposed CLEAR (Coherent Low Energy A (Nuclear) Recoils) experiment will measure coherent elastic neutral current neutrino-nucleus scattering at the SNS. The physics reach includes tests of the Standard Model.

1. Neutrino Production at the SNS

The Spallation Neutron Source (SNS) is a recently-completed facility located at Oak Ridge National Laboratory, TN: it provides the most intense pulsed neutron beams in the world for use in a wide range of science and engineering studies. The beam is pulsed at 60 Hz and the expected power in the first phase is 1.4 MW. First beam was attained in 2006, and the power has been gradually increasing. Full power is expected in 2010. Some upgrades are envisioned for the next decade, including a power upgrade to 2-5 MW, and possibly a second target station.

Neutrinos are produced as a free by-product when protons hit the SNS target. The collisions produce hadronic showers including pions. Whereas π^- get captured, π^+ slow and decay at rest. The $\pi^+ \rightarrow \mu^+ + \nu_\mu$ decay at rest produces a prompt, monochromatic 29.9 MeV ν_μ . The μ^+ then decays on a 2.2 μ s timescale to produce a $\bar{\nu}_\mu$ and a ν_e with energies between 0 and $m_\mu/2$. The $\bar{\nu}_e$ flavor is nearly absent from the flux. See Figures 1 and 2. About 0.13 neutrinos per flavor per proton are expected, which amounts to about 10^7 per flavor at 20 m from the target (Avignone and Efremenko [2003]). The short-pulse time structure of the SNS is also advantageous: for a 60 Hz rate, the background rejection factor is a few times 10^{-4} .

Past experiments have successfully used similar stopped-pion ν sources: examples are LANSCE at LANL, which hosted the LSND experiment (Athanassopoulos et al. [1997]), and ISIS at RAL, which hosted KARMEN (Zeitnitz [1994]). However the SNS has far superior characteristics for neutrino experiments compared to any existing or near-future source.

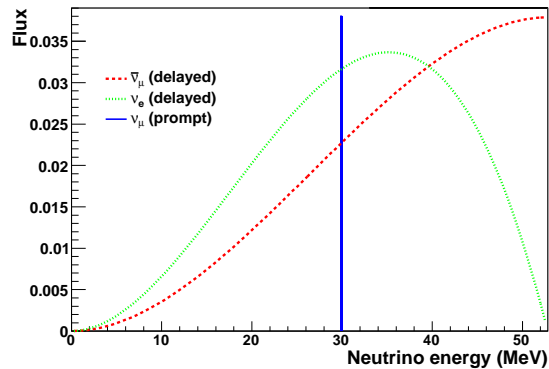


Figure 1: Stopped-pion neutrino spectrum, showing the different flavor components.

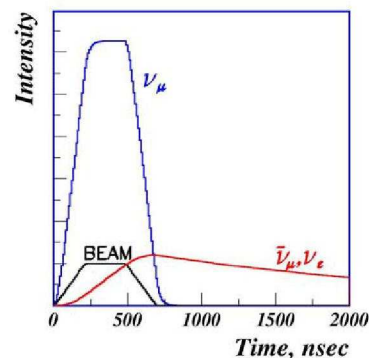


Figure 2: Timing of the SNS pulse with respect to the neutrino fluxes.

2. Coherent Elastic Neutral Current Neutrino-Nucleus Scattering

Coherent elastic neutral current neutrino-nucleus scattering (Freedman et al. [1977]) has never been observed. In this process, a neutrino of any flavor scatters off a nucleus at low momentum transfer Q such that the nucleon wavefunction amplitudes are in phase and add coherently. The cross-section for a spin-zero nucleus, neglecting radiative corrections, is given by (Horowitz et al. [2003]),

$$\left(\frac{d\sigma}{dE}\right)_{\nu A} = \frac{G_F^2}{2\pi} \frac{Q_w^2}{4} F^2(2ME)M \left[2 - \frac{ME}{k^2}\right], \quad (1)$$

where k is the incident neutrino energy, E is the nuclear recoil energy, M is the nuclear mass, F is the ground state elastic form factor, Q_w is the weak nuclear charge, and G_F is the Fermi constant. The condition for coherence requires that $Q \lesssim \frac{1}{R}$, where R is the nuclear radius. This condition is largely satisfied for neutrino energies up to ~ 50 MeV for medium A nuclei. Typical values of the total coherent elastic cross-section are in the range $\sim 10^{-39}$ cm², which is relatively high compared to other neutrino interactions in this energy range (*e.g.* charged current inverse β decay on protons has a cross-section $\sigma_{\bar{\nu}_e p} \sim 10^{-40}$ cm², and elastic neutrino-electron scattering has a cross-section $\sigma_{\nu_e e} \sim 10^{-43}$ cm²).

In spite of its large cross-section, coherent elastic νA scattering has been difficult to observe due to the very small resulting nuclear recoil energies. The maximum recoil energy is $\sim 2k^2/M$, which is in the sub-MeV range for $k \sim 50$ MeV and for typical detector materials (carbon, oxygen). Such energies are below the detection thresholds of most conventional neutrino detectors. However, in recent years there has been a surge of progress in the development of novel ultra-low threshold detectors, many with the aim of WIMP recoil detection or pp solar neutrino detection. Thresholds of ~ 10 keV or even lower may be possible. Some of these new technologies, for instance noble liquids (McKinsey and Coakley [2005]), may plausibly attain ton-scale masses in the relatively near future.

Although ongoing efforts to observe coherent νA scattering at reactors (Barbeau et al. [2007], Collar [2008], Wong et al. [2006]) are promising, a stopped-pion beam has several advantages with respect to the reactor experiments. Higher recoil energies bring detection within reach of the current generation of low threshold detectors which are scalable to relatively large target masses. Furthermore, the pulsed nature of the source (see Figure 2) allows both background reduction and precise characterization of the remaining background by measurement during the beam-off period. Finally, the different flavor content of the SNS flux means that physics sensitivity is complementary.

The expected rates for the SNS are quite promising for noble liquids (Scholberg [2006]): see Figures 3 and 4.

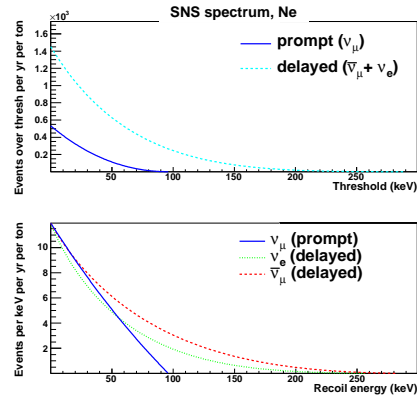


Figure 3: Bottom: Differential yield at the SNS in one ton of Ne (solid: ν_μ , dotted: ν_e , dashed: $\bar{\nu}_\mu$) per year per keV, as a function of recoil energy, for one year of running at the SNS at 46 m from the target. Top: Number of interactions over recoil energy threshold (solid: ν_μ , dashed: sum of ν_e and $\bar{\nu}_\mu$), as a function of recoil energy threshold.

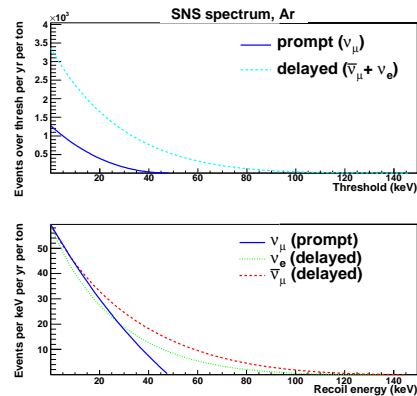


Figure 4: Same as Figure 3 for Ar.

Coherent elastic νA scattering reactions are important in stellar core collapse processes (Freedman et al. [1977]), as well as being useful for core collapse supernova neutrino detection (Horowitz et al. [2003]). A rate measurement will have bearing on supernova neutrino physics. The νA coherent elastic scattering cross-section is predicted by the Standard Model (SM), and form factor uncertainties are small (Horowitz et al. [2003]). Therefore a measured deviation from prediction could be a signature of new physics. Some possibilities are described below.

The SM predicts a coherent elastic scattering rate proportional to Q_w^2 , the weak charge given by $Q_w = N - (1 - 4 \sin^2 \theta_W)Z$, where Z is the number of protons, N is the number of neutrons and θ_W is the weak mixing angle. Therefore the weak mixing angle can be extracted from the measured absolute cross-section, at

a typical Q value of $0.04 \text{ GeV}/c$. A deviation from the SM prediction could indicate new physics. If the absolute cross-section can be measured to 10%, there will be an uncertainty on $\sin^2 \theta_W$ of $\sim 5\%$. One might improve this uncertainty by looking at ratios of rates in targets with different N and Z , to cancel common flux uncertainties; future use of enriched neon is a possibility. There are existing precision measurements from atomic parity violation (Bennett and Wieman [1999], Eidelman et al. [2004]), SLAC E158 (Anthony et al. [2005]) and NuTeV (Zeller et al. [2002]). However there is no previous neutrino scattering measurement in this region of Q . This Q value is relatively close to that of the proposed Q_{weak} parity-violating electron scattering experiment at JLAB (van Oers [2007]). However coherent elastic νA scattering tests the SM in a different channel and therefore is complementary: we note that this is a first-generation experiment.

In particular, one can search for non-standard interactions (NSI) of neutrinos with nuclei. Existing and planned precision measurements of the weak mixing angle at low Q do not constrain new physics which is specific to neutrino-nucleon interactions. The signature of NSI is a deviation from the expected cross-section. Reference (Scholberg [2006]) explores the sensitivity of an experiment at the SNS. As shown in the reference, under reasonable assumptions, if the rate predicted by the SM is observed, neutrino scattering limits more stringent than current ones (Dorenbosch et al. [1986], Davidson et al. [2003]) by about an order of magnitude can be obtained. Reference (Barranco et al. [2007]) looks at the sensitivity of a coherent νA scattering experiment to some specific physics beyond the Standard Model, including models with extra neutral gauge bosons, leptoquarks and R-parity breaking interactions.

Searches for NSI are based on precise knowledge of the nuclear form factors, which are known to better than 5% (Horowitz et al. [2003]), so that a deviation from the SM prediction would indicate physics beyond the SM. If we assume that the Standard Model is a good description, then with sufficient precision one can measure neutron form factors. (Reference (Amanik and McLaughlin [2007]) explores this possibility, which could be within reach of a next-generation experiment.) If a small deviation from the SM prediction were to be observed, presumably one would have to pursue additional measurements to determine whether the discrepancy were due to nuclear physics or beyond-the-SM physics. It would be interesting in either case.

3. The CLEAR Experiment

The specific detector we plan to build is called CLEAR (Coherent Low Energy A (Nuclear) Recoils). We have selected a single-phase design which allows

interchangeable noble liquid target materials. Multiple targets are desirable to test for physics beyond the Standard Model.

The CLEAR experiment at the SNS comprises an inner noble liquid detector placed inside a water tank. The water tank will be instrumented with photomultiplier tubes (PMTs) to act as a cosmic ray veto. An overview diagram of the experiment is shown in Figure 5.

3.1. The Inner Noble Liquid Detector

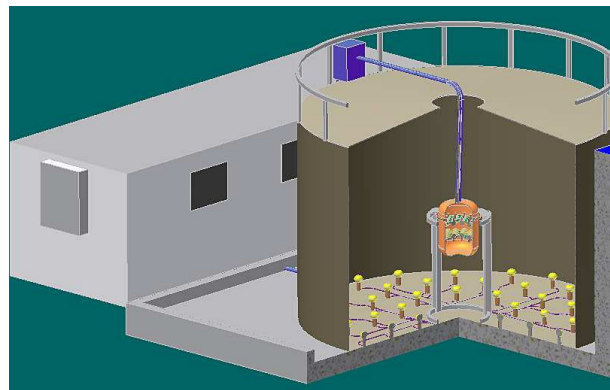


Figure 5: CLEAR experiment concept. The cryogenic inner detector enclosed in a vacuum vessel will be positioned inside a tank of water, which provides neutron shielding and an active muon veto by detection of Cherenkov radiation with an array of PMTs.

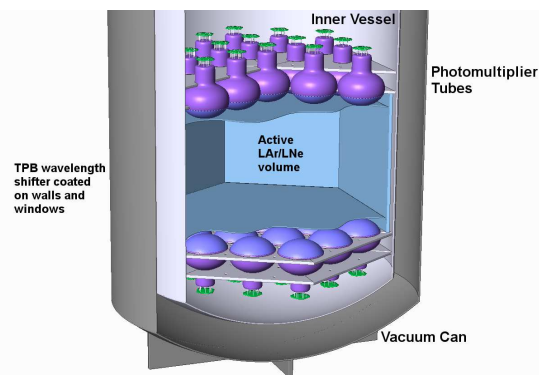


Figure 6: The inner detector, containing an active target of LAr or LNe viewed by photomultipliers, as described in the text.

We propose to use liquid argon (LAr) and liquid neon (LNe) as the detector materials for the first-generation CLEAR experiment. LAr and LNe are bright scintillators, comparable in light yield to NaI but with a faster response. Several properties of LAr and LNe make this overall approach attractive. First, LAr and LNe scintillate strongly in the vacuum ultraviolet and are transparent to their own scintillation

light, allowing for event detection with a low energy threshold. LAr and LNe are dense enough (1.4 and 1.2 g cm^{-3} , respectively) to allow significant target mass in a modest detector volume. Pulse shape discrimination (PSD) to select nuclear recoils is possible because both LAr and LNe have two distinct mechanisms for the emission of scintillation light. These two scintillation channels, resulting from singlet molecule decay and triplet molecule decay, have very different fluorescence lifetimes and are populated differently for electron recoils than for nuclear recoils. This allows nuclear recoils and electron recoils to be distinguished on an event-by-event basis. This approach to electron recoil discrimination has been proposed for liquid neon (McKinsey and Coakley [2005]), and for liquid argon (Boulay and Hime [2006]). Demonstrations of discrimination in the energy window of interest have been accomplished in the MicroCLEAN (Nikkel et al. [2008]), DEAP-I (Boulay et al. [2009]), and WARP (Brunetti et al. [2005]) experiments. The ability to exchange LAr with LNe, with different sensitivities to coherent neutrino scattering and fast neutrons, would allow both event populations to be distinguished and characterized. Finally, argon and neon are relatively inexpensive detector materials.

The CLEAR detector will be a cylindrical LAr/LNe scintillation detector, with an active LAr (LNe) mass of 456 (391) kg. The active volume will be about 60 cm in diameter, and 44 cm tall. A schematic of the active detector is shown in Figure 6. The central active mass will be viewed by 38 Hamamatsu R5912-02MOD photomultipliers (PMTs) divided into two arrays, one on the top of the active volume facing down, and the second array on the bottom facing up. All PMTs will be completely immersed in the cryogenic liquid. A cylinder of PTFE will define the outer radius of the active volume. The bottom and top of the active volume will be defined by two fused silica or acrylic plates. Ionizing radiation events in the liquid cryogen will cause scintillation in the vacuum ultraviolet (80 nm in LNe or 125 nm in LAr), which is too short to pass through the PMT glass. The inner surface of the PTFE walls and end plates will be coated with a thin film of tetraphenyl butadiene (TPB) wavelength shifter. The ultraviolet scintillation light is absorbed by the wavelength shifter and re-emitted at a wavelength of 440 nm. The photon-to-photon conversion efficiency is about 100% for LAr scintillation and about 130% for LNe scintillation (McKinsey et al. [1997]). The wavelength-shifted light is then detected by the PMTs. Using the MicroCLEAN detector we have verified that the chosen PMT model can be used immersed in LAr or LNe.

The detector will be contained in a stainless steel vacuum cryostat. A pulse-tube refrigerator, mounted near the water tank, provides cooling power to maintain the active fluid at the desired temperature value. The noble gas is continuously circulated, boiled, pu-

rified and re-liquefied during operation to maintain a sufficiently large light yield and triplet molecule lifetime. Molecular impurities that affect light collection are removed using gas-phase recirculation through a commercial heated getter. We have found this approach to be highly effective in MicroCLEAN, and it is the same approach used in the XENON (Angle et al. [2008]) and LUX (LUX collaboration [2009]) experiments.

We will calibrate the detector using low-activity neutron sources such as ^{252}Cf or Am/Be to determine the nuclear recoil response, and gamma ray sources such as ^{57}Co and ^{137}Cs to determine the electronic recoil response. Calibration sources will be introduced into the tank from above, inserted down a fixed stainless steel tube until they are adjacent to the cryostat at a known position.

3.2. Siting and Shielding

The CLEAR experiment will occupy a site 46 m from the SNS target, behind the beam (see Figure 7).

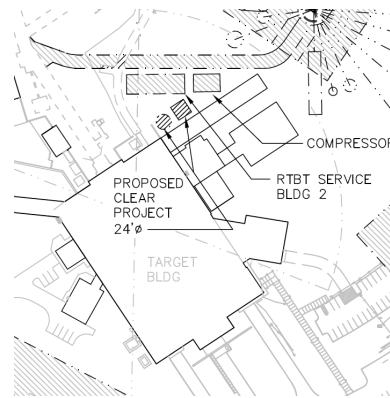


Figure 7: CLEAR site at the SNS.

The detector will sit inside a standard steel agricultural water tank of about 24 ft in diameter and 16 ft in height, which will serve both for shielding and as a cosmic ray veto. Additional steel shielding blocks will also be employed. The water tank will be instrumented with 32 8-inch PMTs. The inside of the tank will be protected against corrosion and lined with Tyvek to increase reflectivity and light collection, as was done for both Super-K (Fukuda et al. [2003]) and KamLAND (Eguchi et al. [2003]) outer detectors. Our Geant4 (Agostinelli et al. [2003], Allison et al. [2006]) simulations show that excellent cosmic veto efficiency is obtained with at least 20 PMTs, and a configuration in which all PMTs are placed on the bottom of the tank is near-optimal.

3.3. Backgrounds

We assume the SNS is running at its full 1.4 MW power, and a live running time of 2.4×10^7 s/yr for each of LAr and LNe. The SNS is expected to be running at full power by early 2010, which is before the anticipated start time of CLEAR. With a nuclear recoil energy window between 20-120 keV (30-160 keV) and a 456 (391) kg LAr (LNe) target, we will have about 890 (340) signal events from the muon decay flux, and about 210 (110) signal events from the prompt ν_μ flux. Backgrounds for the ν signal detection come from neutrons (cosmic and SNS-related) and misidentified gammas.

We divide the backgrounds into two main categories: beam-related and non-beam-related. Inelastic neutrino interaction backgrounds are assumed negligible; not only are cross-sections an order of magnitude smaller than the coherent elastic νA cross-section, but such events will produce electrons or gammas and hence will be rejected by PSD selection. We have adopted several strategies for estimating background. For beam-related background, we make use of simulations done by the SNS neutronics group (Nu-SNS Collaboration [2005], updated December 2007), and further propagate these through the shielding using FLUKA 2008.3b.1 code (Ferrari et al. [2005], Battistoni et al. [2007]). The background event rate is estimated using a Geant4-based inner detector simulation. For cosmic ray-related background, we employed a cosmic-ray generator (Hagmann et al. [2008]) and an independent Geant4 simulation of the water veto tank. The inner detector simulation code was also employed to estimate backgrounds due to radioactivity of the detector materials. These background estimates are discussed in more detail below, and results are summarized in Figures 10 and 11.

Beam-related backgrounds: Beam-related neutrons, which can cause nuclear recoils in the energy region of interest, are of concern because if they occur within the $10 \mu\text{s}$ beam timing window they will be indistinguishable from signal on an event-by-event basis. At SNS beam turn-on in 2006 we began measurements of neutron and gamma fluxes at a site inside the target building using 5 inch liquid scintillator detectors with pulse shape discrimination capabilities. One of these was also used for measurements outside the target building. The measured neutron flux showed little obvious correlation with beam power at the inside site through 2006. These measurements give only a general order of magnitude estimate. We expect changes as the nearby instruments turn on and beam power changes. However, we did observe that the fast neutron flux dropped rapidly with respect to the beam, and was unobservable by our detectors after a few μs .

The dominant beam-related background is neutrons produced from a beam loss of 1 W/m in the transport line. The neutron flux from the SNS target is much

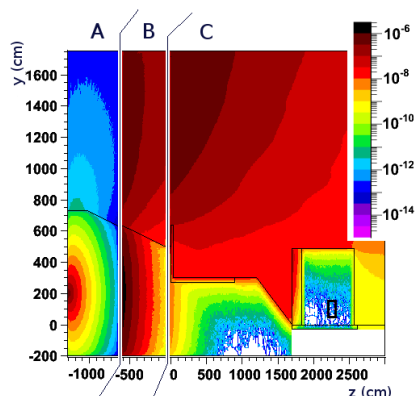


Figure 8: Predicted spatial distribution of neutrons given as a fluence graph (tracklength density, $\text{cm}^2/\text{cm}^3/\text{primary}$). The color scale applies to stage C. Shown is a projection averaging over ± 150 cm with respect to the plane of interest which is perpendicular to the beam line and passes through the center of the CLEAR detector volume.

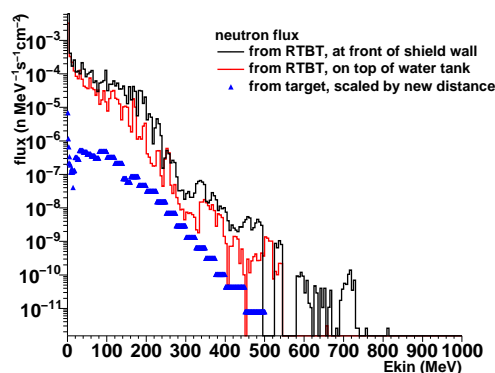


Figure 9: Predicted neutron flux just in front of the iron shield wall (black line) and also for neutrons entering the water tank from the top (red line). For comparison we include the predicted neutron background originating from the SNS target scaled to the CLEAR location.

less than the contribution from the beam line, but has the same spectral shape. Neutrons from the instrumentation also have the same spectral shape, but are highly dependent on the position of the instruments, and cannot be properly evaluated at this time. The beam line is enclosed in an approximately square tunnel with walls 75 cm thick and buried under at least 550 cm of soil. The neutronics group at the SNS has simulated the neutron spectrum directly above beamline and the soil, and at a perpendicular distance of 34 m from the CLEAR detector. We implement in FLUKA a basic 3D model of the site and a radial line source aligned with the beam line. In order to maintain statistical accuracy at the higher neutron energies, we throw neutrons in a flat kinetic energy distribution up to 1 GeV. Later the neutron energy distribution is imposed on the results. The propagation is

accomplished in three stages (as shown in Figure 8) to speed the simulation, and to allow normalization to the neutronics simulation mentioned above. The first stage, A, simulated the beam tunnel and soil for a beam intensity of approximately 1 MW. Figure 9 shows flux in the front of the steel wall and on top of the water tank. The neutron flux into the target volume, as shown in stage C, is a projection onto the plane of the figure from -150 cm behind to 150 cm in front of the plane. The flat neutron spectrum has been filtered by the initial neutron spectrum. The figure shows that almost all of the background comes from “sky shine” and not directly from the beamline. Although not shown, neutrons which leave the beamline with energies below approximately 200 MeV are absorbed in the shielding. Obviously, neutrons with higher energies degrade to lower energies, but with less intensity. The neutrons (and gammas which are not shown) entering the target volume are then passed to the inner detector Geant4 simulation.

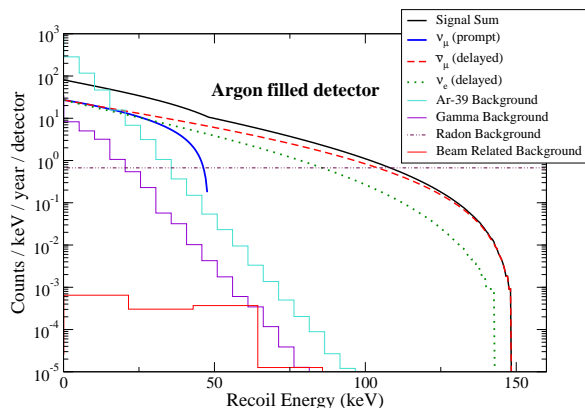


Figure 10: Number of events in both neutrino signals along with beam and detector related backgrounds, for a LAr filled detector (456 kg).

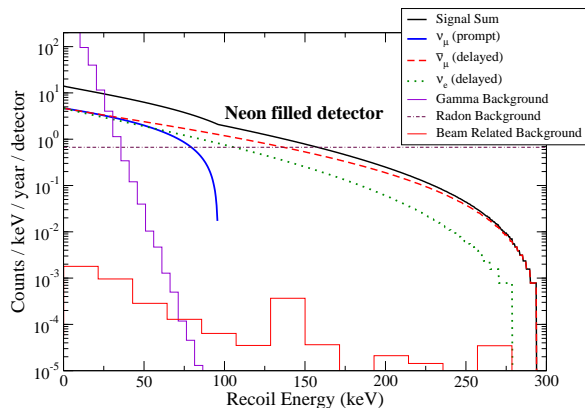


Figure 11: Same as Figure 10 for a LNe filled detector (391 kg).

These beam-related background numbers are our best estimate according to currently known parameters. While they are comfortably small, they still have considerable uncertainties. Furthermore, characteristics of the background are expected to change as nearby instruments turn on and off. For this reason, we plan comprehensive background measurements on-site before detector installation and during running. Based on the pre-installation measurements, we will optimize the shielding configuration. The detector stand will be movable to allow for repositioning of the inner detector within the water tank to allow for minimization of backgrounds. The concrete pad will be designed with driven pilings, so it can accommodate extra shielding if needed. The shielding itself will be available for very low cost in the form of Duratek steel blocks.

Non-beam-related backgrounds: These are mitigated by the SNS beam window: the timing, shown in Figure 1, allows a factor of 6×10^{-4} rejection of steady-state backgrounds assuming a 10 μ s timing window. Timing of individual events in the detector can be known to within ~ 10 ns using the fast scintillation signal. Furthermore, these backgrounds can be subtracted using beam-off data. Cosmic ray-related background can be vetoed with high efficiency by our muon veto phototubes, and ambient radioactivity will be reduced significantly by the water shielding. The estimated rates of cosmic-ray neutrons creating signal candidates during the beam window are small and are not shown in Figures 10 and 11.

We rely on pulse shape discrimination to reduce γ backgrounds. At energies above a few tens of keV, LAr and LNe scintillation detectors are capable of very good discrimination, as described in references Nikkel et al. [2008] and Lippincott et al. [2008]. Gamma backgrounds are dominated by the ^{238}U , ^{232}Th , and ^{40}K that are present in the PMT glass. The contribution due to the stainless steel cryostat and other materials is small in comparison. ^{39}Ar , which is present in atmospheric argon at approximately 1 part in 10^{15} , decays at a rate of about 0.8 Bq/kg of argon. While this is a relatively high rate, PSD is highly efficient at removing this background, improving exponentially with energy. Figure 10 shows that ^{39}Ar background is smaller than the signal above a nuclear recoil energy threshold of 20 keV, given a beam timing cut of 6×10^{-4} . Measurements of the ^{39}Ar rate without beam timing cuts will allow this background to be measured accurately and statistically subtracted. We note that it may be possible to reduce ^{39}Ar background significantly by employing depleted argon from underground sources (Galbiati and Purtschert [2008]). In LNe, electron recoil background is dominated by gamma ray Compton scattering. This occurs at a rate much less than the ^{39}Ar rate in LAr, but the PSD is less effective in LNe, resulting in a higher analysis threshold

of 30 keV.

Radon daughters are another background of concern, which may also be substantially removed using beam timing cuts. In particular, ^{210}Po , which has a 138-day half-life, can produce nuclear recoils in the active volume that can mimic the signal from νA scattering. The inside surface of the active region is approximately 2.9 m^2 in area. By mechanically scrubbing the PTFE and fused silica surfaces before TPB deposition, bagging these pieces in radon-impermeable plastic during the time between deposition and installation, and maintaining these surfaces in a HEPA-filtered atmosphere during final assembly, we expect to be able to keep the radon daughter decay rate below $100\text{ m}^{-2}\text{ day}^{-1}$ in the energy region of interest. This target value for CLEAR exceeds the radon daughter background rate per unit area already demonstrated in the DEAP-I experiment at SNO-LAB (Boulay [2008]), which contains similar TPB-coated acrylic surfaces. The initial surface treatment and TPB coating of the PTFE and fused silica will take place offsite, and final installation will occur in a HEPA-filtered enclosure adjacent to the experimental site at the SNS. After timing cut, radon daughter background corresponds to a background of about 100 events in the year after installation. As in the case of ^{39}Ar background, radon daughter background can be quantified without beam timing to gain an accurate measurement of its rate.

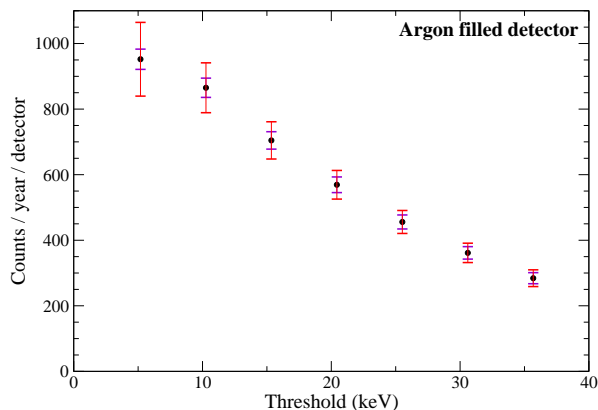


Figure 12: Plots of the integrated signals as a function of analysis threshold, for a LAr filled detector (456 kg). The smaller error bars include just the statistical uncertainties on the signal. The larger error bars incorporate all systematic uncertainties including those due to the background subtraction. The total measured signal is suppressed by a factor of two in these plots due to a flat pulse shape discrimination cut. In the real experiment an energy-dependent cut will preserve more of the signal at higher energies.

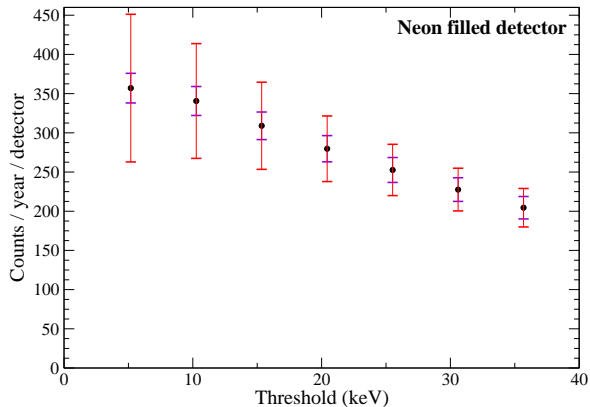


Figure 13: Same as Fig 13 for a LNe filled detector (391 kg).

3.4. Signal and Background Summary

Figures 10 and 11 show the results of the background simulations as compared to the expected signal for both argon and neon. Plotted along with the signal curves (and their sum) are the beam-related backgrounds, the ^{39}Ar backgrounds (for the argon case), an estimate of the radon background, and the gamma background in both LAr and LNe. We note here also that the signal will have a characteristic time-structure (a prompt component with known delay from the SNS target, and a μ decay component of known time constant), distinct from that of the background. After folding in the above backgrounds and the 50% detector efficiency, we can calculate the expected total integrated signal as a function of analysis threshold. This is shown in Figures 12 and 13.

Systematic uncertainties: Assuming one year of data, the statistical uncertainty on the rate measurement is estimated to be 4% (8%) for LAr (LNe). The uncertainty in the neutrino flux is estimated to be 10% and is currently the dominant uncertainty in this measurement. The energy threshold uncertainty also contributes uncertainty to the overall νA scattering cross-section. The analysis threshold is much above the trigger threshold, so the uncertainty in the energy threshold is dominated by uncertainty in the energy scale. The energy scale will be determined through calibration using γ -ray sources in combination with the known LAr and LNe nuclear recoil scintillation efficiencies. Overall we project a systematic uncertainty from energy threshold to be 4% (3%) from LAr (LNe). There is comparatively little uncertainty in the target mass, as there are no fiducial cuts assumed in the analysis, the density of the liquid is well known, and the active volume can be measured accurately during assembly. We estimate the fiducial mass to be calculable with better than 1% uncertainty. Background uncertainties are in the few percent range. Overall expected

uncertainty on the coherent νA rate measurement is 12% (13%) for LAr (LNe).

4. Summary

The SNS creates an intense neutrino source in the few tens of MeV energy range. The CLEAR experiment aims to measure coherent elastic ν -A scattering by siting a single-phase noble liquid scintillation detector 46 m from the SNS neutrino source. The planned active target mass is 456 kg of LAr or 391 kg of LNe. Non-beam-related backgrounds include cosmic rays, internal and external radioactivity, radon, and ^{39}Ar (for argon); all of these may be well characterized using data outside of the beam window. Beam-related neutron backgrounds, which cannot be rejected using the beam time window, have been shown using extensive simulations to be comfortably small. The absolute rate can be measured with ~ 12 -13% uncertainty.

Acknowledgments

The CLEAR collaboration is grateful to the SNS neutronics group for background simulations.

References

- F. T. Avignone and Y. V. Efremenko, *J. Phys.* **G29**, 2615 (2003).
- C. Athanassopoulos et al. (LSND), *Nucl. Instrum. Meth.* **A388**, 149 (1997), nucl-ex/9605002.
- B. Zeitnitz (KARMEN), *Prog. Part. Nucl. Phys.* **32**, 351 (1994).
- D. Z. Freedman, D. N. Schramm, and D. L. Tubbs, *Ann. Rev. Nucl. Part. Sci.* **27**, 167 (1977).
- C. J. Horowitz, K. J. Coakley, and D. N. McKinsey, *Phys. Rev.* **D68**, 023005 (2003), astro-ph/0302071.
- D. N. McKinsey and K. J. Coakley, *Astropart. Phys.* **22**, 355 (2005), astro-ph/0402007.
- P. S. Barbeau, J. I. Collar, and O. Tench, *JCAP* **0709**, 009 (2007), nucl-ex/0701012.
- J. I. Collar (CoGeNT), *J. Phys. Conf. Ser.* **136**, 022009 (2008).
- H. T. Wong, H.-B. Li, J. Li, Q. Yue, and Z.-Y. Zhou, *J. Phys. Conf. Ser.* **39**, 266 (2006), hep-ex/0511001.
- K. Scholberg, *Phys. Rev.* **D73**, 033005 (2006), hep-ex/0511042.
- S. C. Bennett and C. E. Wieman, *Phys. Rev. Lett.* **82**, 2484 (1999), hep-ex/9903022.
- S. Eidelman et al. (Particle Data Group), *Phys. Lett.* **B592**, 1 (2004).
- P. L. Anthony et al. (SLAC E158), *Phys. Rev. Lett.* **95**, 081601 (2005), hep-ex/0504049.
- G. P. Zeller et al. (NuTeV), *Phys. Rev. Lett.* **88**, 091802 (2002), hep-ex/0110059.
- W. T. H. van Oers (Qweak) (2007), arXiv:0708.1972 [nucl-ex].
- J. Dorenbosch et al. (CHARM), *Phys. Lett.* **B180**, 303 (1986).
- S. Davidson, C. Peña Garay, N. Rius, and A. Santamaria, *JHEP* **03**, 011 (2003), hep-ph/0302093.
- J. Barranco, O. G. Miranda, and T. I. Rashba, *Phys. Rev.* **D76**, 073008 (2007), hep-ph/0702175.
- P. S. Amanik and G. C. McLaughlin (2007), arXiv:0707.4191 [hep-ph].
- M. Boulay and A. Hime, *Astroparticle Physics* **25**, 179 (2006).
- J. A. Nikkel, R. Hasty, W. H. Lippincott, and D. N. McKinsey, *Astroparticle Physics* **29**, 161 (2008).
- M. G. Boulay et al. (2009), 0904.2930.
- R. Brunetti, E. Calligarich, M. Cambiaghi, F. Carbonara, A. Cocco, C. D. Vecchi, R. Dolfini, A. Ereditato, G. Fiorillo, and L. Grandi, *New Astronomy Reviews* **49**, 265 (2005), URL <http://www.sciencedirect.com/science/article/B6VNJ-4FGXS7>.
- D. N. McKinsey, C. R. Brome, J. S. Butterworth, R. Golub, K. Habicht, P. R. Huffman, S. K. Lamoreaux, C. E. H. Mattoni, and J. M. Doyle, *Nuclear Instruments & Methods in Physics Research Section B-Beam Interactions with Materials and Atoms* **132**, 351 (1997).
- J. Angle et al. (2008), 0805.2939.
- LUX collaboration (2009), URL <http://lux.brown.edu/>.
- Y. Fukuda et al., *Nucl. Instrum. Meth.* **A501**, 418 (2003).
- K. Eguchi et al. (KamLAND), *Phys. Rev. Lett.* **90**, 021802 (2003), hep-ex/0212021.
- S. Agostinelli et al. (GEANT4), *Nucl. Instrum. Meth.* **A506**, 250 (2003).
- J. Allison et al., *IEEE Trans. Nucl. Sci.* **53**, 270 (2006). Nu-SNS Collaboration (2005), URL <http://www.phy.ornl.gov/nusns/proposal.pdf>.
- A. Ferrari, P. R. Sala, A. Fassò, and J. Ranft, CERN yellow report (2005), URL <http://doc.cern.ch/yellowrep/2005/2005-010/cern2005-010.pdf>.
- G. Battistoni et al., *AIP Conf. Proc.* **896**, 31 (2007).
- C. Haggmann, D. Lange, and D. Wright (2008), URL <http://nuclear.llnl.gov/simulation/>.
- W. H. Lippincott, K. J. Coakley, D. Gastler, A. Hime, E. Kearns, D. N. McKinsey, J. A. Nikkel, and L. C. Stonehill, *Phys. Rev. C* **78**, 035801 (2008), URL <http://link.aps.org/abstract/PRC/v78/e035801>.
- C. Galbiati and R. Purtschert, *J. Phys. Conf. Ser.* **120**, 042015 (2008), 0712.0381.
- M. Boulay, Proceedings of IDM 2008, Stockholm (2008).